Received: 24 May 2019 | Revised: 20 October 2019 | Accepted: 22 October 2019

DOI: 10.1096/fj.201901314RR

RESEARCH ARTICLE

THE FASEB JOURNAL

Tracheal brush cells release acetylcholine in response to bitter tastants for paracrine and autocrine signaling

Monika I. Hollenhorst[1] | Innokentij Jurastow[2,3] | Rajender Nandigama[4] | Silke Appenzeller[5] | Lei Li[6] | Jörg Vogel[7] | Stephanie Wiederhold[2] | Mike Althaus[8] | Martin Empting[9,10,11] | Janine Altmüller[12] | Anna K. H. Hirsch[9,10,11] | Veit Flockerzi[13] | Brendan J. Canning[14] | Antoine-Emmanuel Saliba[7] | Gabriela Krasteva-Christ[1]

[1]Institute of Anatomy and Cell Biology, Saarland University, Homburg, Germany

[2]Institute of Anatomy and Cell Biology, Justus-Liebig-University of Giessen, Giessen, Germany

[3]Department of Anesthesiology and Intensive Care Medicine (CS), University Hospital Charité, Humboldt University of Berlin, Berlin, Germany

[4]Institute of Anatomy and Cell Biology, University of Würzburg, Würzburg, Germany

[5]Comprehensive Cancer Centre Mainfranken, University of Würzburg, Würzburg, Germany

[6]Core Unit SysMed, University of Würzburg, Würzburg, Germany

[7]Helmholtz Institute for RNA-based Infection Research (HIRI), Helmholtz-Centre for Infection Research (HZI), Würzburg, Germany

[8]School of Natural and Environmental Sciences, Newcastle University, Newcastle upon Tyne, United Kingdom

[9]Department of Drug Design and Optimization (DDOP), Helmholtz-Institute for Pharmaceutical Research Saarland (HIPS)-Helmholtz Centre for Infection Research (HZI), Saarbrücken, Germany

[10]Department of Pharmacy, Saarland University, Saarbrücken, Germany

[11]German Centre for Infection Research (DZIF), Saarbrücken, Germany

[12]Cologne Centre for Genomics, University of Cologne, Cologne, Germany

[13]Institute of Experimental and Clinical Pharmacology and Toxicology/PZMS, Saarland University, Homburg, Germany

[14]Department of Medicine, Division of Allergy and Clinical Immunology, School of Medicine, Johns Hopkins University, Baltimore, MD, USA

Correspondence
Gabriela Krasteva-Christ, Saarland University, Institute of Anatomy and Cell Biology, UKS, Gebäude 61, 66421 Homburg, Germany.
Email: Gabriela.Krasteva-Christ@uks.eu

Funding information
German Research Society, Grant/Award Number: DFG SFB TRR 152; Helmholtz Association's Initiative and Networking Fund

Abstract

For protection from inhaled pathogens many strategies have evolved in the airways such as mucociliary clearance and cough. We have previously shown that protective respiratory reflexes to locally released bacterial bitter "taste" substances are most probably initiated by tracheal brush cells (BC). Our single-cell RNA-seq analysis of murine BC revealed high expression levels of cholinergic and bitter taste signaling transcripts (*Tas2r108*, *Gnat3*, *Trpm5*). We directly demonstrate the secretion of acetylcholine (ACh) from BC upon stimulation with the Tas2R agonist denatonium. Inhibition of the taste transduction cascade abolished the increase in $[Ca^{2+}]_i$ in

Abbreviations: 2-AA, 2-aminoacetophenone; ACh, acetylcholine; BC, brush cells; ChAT, choline acetyltransferase; DHQ, 2,4-dihydroxyquinoline; FPKM, fragments per kilobase of exon model per million reads mapped; MC, mucociliary clearance; MR, muscarinic acetylcholine receptor; nAChR, nicotinic acetylcholine receptor; PCA, principal component analysis; PQS, Pseudomonas quinolone signal; PTS, particle transport speed; QSM, quorum sensing molecule; SCDE, single-cell differential expression; TasR, taste receptor; TRPM5, transient receptor potential melastatin 5.

Monika I. Hollenhorst, Innokentij Jurastow and Rajender Nandigama contributed equally to this work.

BC and subsequent ACh-release. ACh-release is regulated in an autocrine manner. While the muscarinic ACh-receptors M3R and M1R are activating, M2R is inhibitory. Paracrine effects of ACh released in response to denatonium included increased $[Ca^{2+}]_i$ in ciliated cells. Stimulation by denatonium or with *Pseudomonas* quinolone signaling molecules led to an increase in mucociliary clearance in explanted tracheae that was Trpm5- and M3R-mediated. We show that ACh-release from BC via the bitter taste cascade leads to immediate paracrine protective responses that can be boosted in an autocrine manner. This mechanism represents the initial step for the activation of innate immune responses against pathogens in the airways.

KEYWORDS

acetylcholine, brush cells, mucociliary clearance, single-cell RNA-seq, taste

1 | INTRODUCTION

The airway epithelium is constantly exposed to inhaled potentially harmful exogenous substances and pathogens. However, absence or very low levels of inflammation indicate the presence of innate sensing mechanisms that can either signal "keep calm" or initiate protective responses such as secretion of antimicrobial peptides, a boost in mucociliary clearance (MC) or neurogenic inflammation.[1-3] The first barrier defense to xenobiotics occurs in the mucosal layer of the airways and likely involves epithelial cells and cells of the immune system. In recent years, brush cells (BC), a less abundant epithelial cell type with a characteristic tuft of apical microvilli and elusive function for more than 60 years after their discovery, were identified as specialized chemosensory cells serving as sentinels in various organs including the airway epithelium.[4-8] Based on the recent advances in single-cell RNA-sequencing it became evident that more than one BC type exists in the airways and BC signature varies in different organs.[4,9-11]

In a bacterial artificial chromosome (BAC)-transgenic mouse model expressing eGFP under control of the promoter for the acetylcholine (ACh) synthesizing enzyme choline acetyltransferase (ChAT) and utilizing ChAT-antisera, eGFP-fluorescent tracheal epithelial cells were identified as BC.[7,12] Yet, it remains elusive if these cells indeed synthesize and release ACh. A subtype of type II cells in lingual taste buds are cholinergic and indeed release ACh upon stimulation, which enhances $[Ca^{2+}]_i$ via muscarinic ACh receptors (MR) in an autocrine manner.[13] Cholinergic signaling is important for several innate immune processes in the airways, including MC.[14-17] In the human upper airways nitric oxide released in response to taste receptor (TasR) stimulation increases ciliary beat,[18-21] but there is no proof that the same mechanism operates in the lower airways or additional mechanisms are influencing MC. However, cholinergic signaling is important for other innate immune responses in the upper airways, since activation of solitary chemosensory cells (SCC) leads to cholinergic-mediated neurogenic inflammation in the nose.[22] In the lower airways, cholinergic signaling regulates MC.[16] Thus, it is tempting to speculate, that ACh released from BC in response to TasR signaling could be the major source for regulating MC and respiratory reflexes in lower airways, thereby representing an important regulator of innate immunity in the airways.

Previously, we have shown that a subpopulation of tracheal BC express key molecules of the bitter (Tas2R-coupled) taste signaling cascade, including the G-protein α-gustducin, phospholipase C beta 2 (PLCβ2), and the transient receptor potential melastatin 5 (Trpm5) channel.[7,23] Within the last year, a few groups published RNA-sequencing data on tracheal epithelial cells and specifically on BC.[4,9-11,24] While expression of some transcripts varies in these studies, it is clear, that BC, also called tuft cells, indeed represent a distinct epithelial cell population which is characterized by the expression of taste transduction members.[4,9-11] This suggests that tracheal BC are able to recognize bitter substances. Interestingly, bacterial quorum sensing molecules (QSM), used by bacteria to measure population density, and other bacterial metabolites such as cycloheximide display characteristics of bitter substances. We previously demonstrated that cycloheximide and QSM (N-3-oxododecanoyl-homoserine lactone) act on bitter taste receptors in tracheal BC and evoke protective respiratory reflexes that are epithelium-mediated and dependent on activation of nicotinic ACh receptors (nAChR).[7,25] Sequencing data from ChAT-eGFP-expressing epithelial cells show that these cells are the major source for cysteinyl leukotriene synthesis in the tracheal epithelium and play an important role in allergic inflammation.[4]

Here, we performed single-cell RNA-seq transcriptome analysis of cholinergic brush and ciliated cells to characterize the molecular profile of these distinct cell populations and to gain profound insight in the detection spectrum of BC. We hypothesize, that ACh is released from tracheal BC upon

activation of the classical bitter taste signaling cascade, subsequently evoking protective innate immune effects. We here investigated, if tracheal BC are equipped with an autoregulatory machinery for ACh-release, by studying the ACh-release from these cells in vivo using ACh-sensor cells positioned in their vicinity. Additionally, we investigated the regulation of ACh-release and explored autocrine ACh-signaling on BC using inhibitors and muscarinic receptor (MR)-knockout mouse strains. Paracrine effects on respiration due to released ACh were studied in an in vivo mouse model, as an example for induction of protective reflex responses. The influence of BC-released ACh on particle transport speed (PTS) was studied ex vivo as an example for ACh-mediated innate immune responses.

2 | MATERIALS AND METHODS

2.1 | Animals

Experiments were performed on 8- to 20-week-old ChAT-eGFP,[12] C57Bl6/J mice, and *Trpm5*-deficient mice (provided by Dr V. Chubanov). Additionally, MR subtype 1 (M1R), M3R-, M4R-, and M5R-deficient mice and M2R/M3R double-deficient mice aged between 15 and 40 weeks were used. N-values are displayed in the respective figures. Mice from either sex were kept under specified pathogen-free conditions in accordance with the German and American guidelines for care and use of laboratory animals. Experimental procedures were approved by the Johns Hopkins University Medical School Institutional Animal Care and Use Committee, USA, and the Animal Welfare Committee of the Regional Council in Giessen, Germany. Mice were killed by inhalation of an overdose of isoflurane (Abbott). For in vivo experiments, mice were anesthetized with urethane (1.5 g/kg i.p.) and sacrificed by CO_2 inhalation at the end of the experiment.

2.2 | Single-cell isolation

Tracheae of ChAT-eGFP mice were dissected, cut into small rings and incubated for 30 minutes at 37°C in enzyme buffer containing 2 mg/mL papain, 25 µL/mL L-Cysteine and 0.5 µL DNaseI (Thermo Fisher Scientific) in Tyrode I solution.[2] Tracheal rings were mechanically dissociated. The digestion was stopped by addition of 2 µL leupeptin in 1 mL Tyrode II solution (1 mmol/L $CaCl_2$ in Tyrode I buffer). The tissue was centrifuged, the supernatant removed and the pellet resuspended in Hank's balanced salt solution (HBSS). The cell suspension was placed on coverslips which were transferred to a microscope 30 minutes later. BC were identified by GFP fluorescence and ciliated cells by ciliary beating. Single cells were harvested into a fire-polished borosilicate glass pipette (tip diameter around 100 µm) by applying negative pressure, transferred into a PCR tube containing 1.5 µL RNAse inhibitor (RNAseOUT, 2 U/µL) and immediately frozen at −20°C. If not specified otherwise, all reagents were purchased from Sigma-Aldrich, Taufkirchen, Germany.

2.3 | Single-cell RNA-seq

For preamplification of cDNA from single cells, the SeqPlex™ RNA amplification kit (Sigma-Aldrich) was used. Isolated single cells in RNAse inhibitor were incubated with 0.5 µL library synthesis solution at 70°C for 5 minutes. Denatured RNA was reverse transcribed and the resulting cDNA library amplified according to the manufacturer's protocol. Products were purified using the GenElute PCR Clean-up kit (Sigma-Aldrich) according to the manufacturer's protocol and sequenced.

2.4 | Sequencing and data analysis

The Illumina Nextera® XT DNA sample preparation protocol (Part# 15031942 Rev. C) was used for library preparation, starting with an input amount of 1 ng cDNA following manufacturer's recommendations. After validation (Agilent 2200 TapeStation) and quantification (Invitrogen Qubit System, Thermo Fisher Scientific) all transcriptome libraries were pooled. The pool was quantified using the Peqlab KAPA Library Quantification Kit (VWR) and the Applied Biosystems 7900HT Sequence Detection (Thermo Fisher Scientific). A one paired-end run of 2 × 75bp was performed on the Illumina MiSeq sequencer (Illumina) using v3 chemistry.

Cells were sequenced to a depth of 4.6 ± 0.3 million read pairs. Illumina adapters were removed using Trim Galore (v0.4.0) (https://www.bioinformatics.babraham.ac.uk/projects/trim_galore/) with cutadapt (v1.8).[26] The quality threshold was set to 30. Trimmed reads with a minimum length of 30 bps were mapped to the mouse genome reference sequence (GRCm38.p3) and alignment was performed with STAR (v2.4.0d)[27] using the outSAMstrandField intronMotif option. FPKM (fragments per kilobase of exon model per million reads mapped) values were calculated with Cufflinks (v2.2.1)[28] using the no-effective-length-correction and compatible-hits-norm options. All single cells were subjected to a principal component analysis (PCA, prcomp function of R's stats-package v3.4.4) including genes with an FPKM > 5 in at least two samples and a coefficient of variation >0.5.

A Bayesian-based method SCDE (single-cell differential expression)[29] was used to identify the differentially expressed genes between groups of individual cells. Empirical p-values were calculated based on distribution of SCDE generated

Z-scores. The final genes with a significant *P*-value (<.05) were identified and plotted in a heatmap.

2.5 | Single-cell RT-PCR

Four µL of amplified single-cell cDNA was added to 2.5 µL PCR buffer II, 2 µL 25 mmol/L $MgCl_2$, 0.5 µL dNTP (10 mmol/L each), 0.2 µL AmpliTaq Gold polymerase, 1 µL primer and 14.8 µL H_2O. RT-PCR was performed using gene specific primers (Table 1). The thermal cycler program included initial denaturation for 10 minutes at 95°C followed by 40 cycles of 30 seconds at 95°C, 2 seconds at 60°C, and 20 seconds at 72°C followed by 7 minutes at 72°C. PCR products were separated on a 2% agarose gel and visualized using ethidium bromide fluorescence.

2.6 | Immunohistochemistry

Tissue from ChAT-eGFP mice used for immunohistochemistry was fixed by transcardiac perfusion with Zamboni solution (2% paraformaldehyde (PFA)/15% saturated picric acid in 0.1 mol/L phosphate buffer, pH 7.4). The tissue was thoroughly washed for 3 days and incubated overnight in 18% saccharose dissolved in 0.1 mol/L phosphate buffer. Tracheas were orientated on a piece of filter paper and frozen in melting isopentane. Tracheae were cut into 10 µm cryosections, air-dried and incubated for 1 hour with blocking solution containing 10% normal horse serum, 0.5% Tween 20 and 0.1% BSA in PBS, pH 7.4. The anti-eGFP primary antibody in combination with the other primary antibodies (details in Table S3) diluted in 5 mmol/L phosphate buffer and 4.48 g/L NaCl was applied overnight at room temperature. Sections were washed in PBS and the following secondary antibodies were applied for 1 hour at room temperature: FITC-conjugated donkey anti-chicken IgG (diluted 1:400, Jackson ImmunoResearch), Cy3-conjugated donkey anti-goat IgG (diluted 1:500, Merck Millipore), and Cy3-conjugated donkey anti-rabbit (diluted 1:1000, Merck Millipore). Slides were mounted and evaluated with an epifluorescence microscope (Imager M2, Zeiss).

2.7 | Calcium imaging experiments

Calcium imaging experiments were performed using either ChAT-eGFP mice or M1R-, M2/M3R-, M3R-, M4R-, and M5R-deficient mice. Epithelial cell isolation was performed as described for single-cell picking, with an enzyme buffer consisting of 2 mg/mL dispase II in Ca^{2+}- and Mg^{2+}-free HBSS (Sigma-Aldrich). M3R overexpressing CHO-K1 cells were used as ACh-sensor cells (CRL-1981, ATCC). Cells were cultured in Ham's F12K medium containing 2 mmol/L L-glutamine and 1.5 g/L sodium bicarbonate supplemented with 0.1 mg/mL G418 (90%) and 10% fetal bovine serum (ATCC).

For measurements of paracrine cholinergic signaling of BC, reporter cells were preincubated with the Ca^{2+}-indicator calcium orange AM (5 µmol/L, Invitrogen). Isolated tracheal epithelial cells were mixed with calcium orange loaded sensor cells and were seeded on coverslips. All cells were then loaded with fura-2 AM (5 µmol/L) and sulfobromophthaleine (100 µmol/L, Sigma-Aldrich). Test stimuli were denatonium (1 mmol/L), ATP (100 µmol/L), and ACh (1 µmol/L or 10 µmol/L). The inhibitors atropine (50 µmol/L), TPPO (100 µmol/L), and U73221 (10 µmol/L) were added to the cells 3 minutes prior to the first stimulus. Cells were excited alternatively at 340/380 nm with light from a xenon arc lamp passed through a monochromator (TiLL Photonics), fluorescence emission was detected using a CCD camera and the fluorescence ratio was analyzed using an image analysis software (TiLL Vision, TiLL Photonics). BC and ACh-sensor cells were identified by their respective fluorescence at 488 nm and 580 nm before experiments started.

For investigation of autocrine ACh-signaling in BC, cell suspensions were immunolabeled for Trpm5 (rb-anti-TRPM5 antibody, 1:60, abcam) in 20 µL of HBSS-medium for 45 minutes at 37°C. Cells were washed and transferred onto Cell Tak coated coverslips (according to manufacturer's recommendations). The coverslips were incubated with AlexaFluor488-conjugated goat anti-rabbit IgG (1:500) diluted in Tyrode II buffer containing calcium orange (5 µmol/L) and sulfobromophthaleine (100 µmol/L) for 15 minutes at 37°C. Afterwards the coverslips were placed on the microscope and superfused with warmed Tyrode III solution. The cells on each coverslip were exposed to 12.5 mmol/L denatonium. For characterization of MRs in BC from wild-type mice, experiments were performed with the cholinergic inhibitors atropine (50 µmol/L), gallamine (10 µmol/L), and 4-DAMP (100 nmol/L).

2.8 | ACh-release in whole tracheal preparations

For simultaneous measurements of $[Ca^{2+}]_i$ in BC and ACh-sensor cells, tracheae were explanted and divided into four pieces. Each piece was placed on a cover slip with plated ACh-sensor cells and loaded with calcium orange AM and sulfobromophthaleine as described above. $[Ca^{2+}]_i$ was analyzed using a confocal laser scanning microscope and appropriate software (LSM 710, Zeiss). The imaging speed was 1.57 frames/s. Calcium Orange was excited at 549 nm and fluorescence emission was recorded at 576 nm. BC were identified by their GFP-fluorescence at 488 nm.

TABLE 1 Sequences of the primers used for single-cell RT-PCR of isolated tracheal brush cells from ChAT-eGFP mice

Name	Accession No.	Sequence	Product length (bp)
α-gustducin	NM001081143	fwd tcatccataagaatggttacagc rev cccacagtcgtttaatgatttc	231
PLCβ2	NM177568	fwd tccagatgtttcctgctga rev gggaagtcctctgggttgat	101
GFP	EU056363	fwd acgtaaacggccacaagttc rev aagtcgtgctgcttcatgtg	187
ChAT	NM009891	fwd gaccagctaaggtttgcagc rev caggaagccggtatgatgaga	163
TRPM5	NM020277	fwd tgaggaacgacctttggcta rev acacggatcttggtggatgt	183
Tas2R105	NM020501	fwd gactggcttccttctcatcg rev gcaaacaccccaagagaaaa	284
Tas2R108	NM020502	fwd tggatgcaaacagtctctgg rev ggtgagggctgaaatcagaa	158
β2-MG	NM009735	fwd attcacccccactgagactg rev gctatttctttctgcgtgcat	192
Tas2r102	NM199153	fwd acaggcgacgctgttatatgc rev gcttttgtttaatgacccagtcc	158
Tas2r103	NM053211	fwd agcacagtggcccacataaa rev tggcctgtgggaaaagctac	167
Tas2r104	NM207011	fwd ctgagcgtttggtttagcacc rev ttcacagctagcggaaagga	167
Tas2r106	NM207016	fwd agcctcaacctcttctatctcc rev tcactgtttgtgggaaagcaa	145
Tas2r107	NM199154	fwd tgctcggagtttttaggggaca rev ccagaggtaagcatgtgtggaa	184
Tas2r109	NM207017	fwd tactggtgtctctggtcctctt rev gggacaaaacaacggggaca	186
Tas2r110	NM199155	fwd agcatttcatcagcggatcag rev gcatgtggcaagccaaacg	189
Tas2r113	NM207018	fwd tggcaattagcagaatcgctc rev gatgctcaagtttgcagtaagc	164
Tas2r114	NM207019	fwd cttcctgatagggtgcttgct rev ttgattccatctgcctgcga	242
Tas2r115	NM207020	fwd agactgtggttgccttcctc rev gttttctcacgcttgcacca	229
Tas2r116	NM053212	fwd cttttgctgtgtcactggtca rev tctgatgtgggccttagtgct	119
Tas2r117	NM207021	fwd ggcccacttcaaagccctac rev gctgcgataatacagagaggca	228
Tas2r118	NM207022	fwd tccagcctgaaagctcagttc rev agggttgctcatcatcagtga	195
Tas2r119	NM020503	fwd cgatgctctccattctgtca rev tgatgagtagcaggcactgg	289
Tas2r120	NM207023	fwd atggcaaaggatgtcaagatcag rev atgacctgctgggtagaagga	182
Tas2r121	NM207024	fwd gaacgagaccccagcactaa rev gtcatcacccaaagactggct	236
Tas2r122	NM001039128	fwd tgtggcaagctccattcttga rev acctccacaatgacacaccag	163
Tas2r123	NM207025	fwd tgcaggtcaatgccaaacaac rev tggcttgtctcagcttactgt	243
Tas2r124	NM207026	fwd ctagtgctacggcccacaga rev acatcccagctgcctcatta	239
Tas2r125	NM207027	fwd ggtagtggcctttctcctgtt rev agggaaccaacatccgtaca	233
Tas2r126	NM207028	fwd tcttgttgggctctatcttggt rev gcgaatgccttctgagagaac	240
Tas2r129	NM207029	fwd tggtttcagggactttgctca rev gcaggagaaaagtggactggg	219
Tas2r130	NM199156	fwd tccagacacctacaacagagg rev cagggagataatcacacatgcc	211
Tas2r131	NM207030	fwd gcagtatttataactggaatgctgg rev aggcgctagttcttgtatggt	177
Tas2r134	NM199158	fwd atggcggcctgtgaaaacta rev gtgagcctgggtgctgtaat	207
Tas2r135	NM199159	fwd cagcctctcgattctgtctcc rev aggcaacctgtactttagcca	227
Tas2r136	NM181276	fwd gtgcttcaacccacattaaggt rev aaatcaggtggattggttcctc	132
Tas2r137	NM001025385	fwd acatcagactgaagcgacagg rev ggcctcagcactctgatctc	176
Tas2r138	NM001001451	fwd acgtggtgtcattctgtgct rev tctatggccctcctcagctt	160
Tas2r139	NM181275	fwd ttcgtcgcaacagctactct rev tgttggatgtggacagaagca	184
Tas2r140	NM021562	fwd ccagcaccacagcccatatt rev ttaggacacaagagtggccc	183
Tas2r143	NM001001452	fwd aagcgaaccttattggcatcc rev agcctgggaactaactgggaa	157
Tas2r144	NM001001453	fwd gtgggtgccatcaaatcgac rev atgaacatggtgctgaaaccg	219

Stimulation was carried out with 1 mmol/L or 12.5 mmol/L denatonium and 10 μmol/L ACh. Changes in $[Ca^{2+}]_i$ in sensor cells in proximity to BC were measured by z- and time-lapse series.

For studying the dependency of ACh-release on Trpm5 we explanted tracheae and divided them into two pieces. Each piece was positioned on a coverslip in close proximity to ACh-sensor cells. Loading and measurements

of ACh-sensor cells were performed as described above. Tracheae of wild-type or *Trpm5*$^{-/-}$ mice were stimulated with 1 mmol/L denatonium and 100 µmol/L ACh. After an incubation time of 5 minutes the applied substances were washed out for 5 minutes.

2.9 | Particle transport speed measurements

Particle transport speed (PTS) experiments were performed as described previously.[7,16,30] Tracheae were dissected, mounted under a microscope (Olympus BX 51WI, Olympus GmbH) and 2.3 µL Dynabeads (Invitrogen Dynal AS) were added. Films were recorded with a SMX-150M camera (Sumix Corporation), particles were tracked with the imaging software Stream Pix (Norix Inc) and PTS was evaluated. Baseline was recorded at defined time points starting 30 minutes after the death of the animal and stimulation was performed at min 60. Inhibitors of cholinergic signaling were administered 4 minutes prior to stimulation. Viability of the tissue was verified by application of ATP at min 74. The following substances were used: ACh (100 µmol/L), ATP (100 µmol/L), denatonium (1 mmol/L), atropine (50 µmol/L or 100 µmol/L), mecamylamine (100 µmol/L), 4-DAMP (1 µmol/L), gallamine (10 µmol/L), carbenoxolone (100 µmol/L) and the *P aeruginosa* QSM PQS (100 µmol/L), 2-AA (100 µmol/L), and DHQ (100 µmol/L).

2.10 | Monitoring of the respiratory function

Respiratory function was measured as described previously.[7] Briefly, lungs were cannulated after exposing the trachea and spontaneous breathing of anesthetized mice was monitored over a period of 5 minutes, whereas the tracheal mucosa was perfused with Krebs buffer to establish baseline conditions. A solution containing denatonium (1 mmol/L) was administered in mice with intact tracheal epithelium or mechanically removed epithelium. Application of capsaicin (10 µmol/L) at the end of the experiment served as a positive control for the integrity of nerve fibers in the tracheal mucosa. Additionally, vehicle control experiments (Krebs) and experiments with the nAChR antagonist mecamylamine (100 µmol/L) were performed. For the duration of the experiment, all respiratory events were recorded with a pressure transducer (Biopac MP100) that was connected to a chamber with the mouse thorax. After the experiment, mice were killed by cervical dislocation. Then the integrity of the tracheal epithelium was evaluated as described previously.[7]

2.11 | Statistical analysis

Statistical analysis was performed using the software SPSS 19.0 or GraphPad Prism version 8. All data in the figures are expressed as mean ± SEM except the box plots. Median, upper, and lower quartiles as well as maximum and minimum values are presented in boxplots. Data were analyzed for normal distribution with the Shapiro-Wilk test (PTS experiments) or Kolmogorov-Smirnov test. Peak values before and after application of denatonium or ACh, without or with blocker addition were analyzed with the two-tailed unpaired or paired Student's *t* test where appropriate. To compare multiple groups, one-way factorial ANOVA followed by Dunnett's multiple comparisons test was performed. $P \leq .05$ were considered statistically significant.

3 | RESULTS

3.1 | Unbiased transcriptome analysis of single ChAT-eGFP-positive cells delineated them as a subpopulation of BC

For transcriptome characterization of cholinergic BC, we performed full-length single-cell RNA-seq (Figure S1A,B) in biological replicates of manually picked single ChAT-eGFP positive cells compared to single ciliated cells from dissociated tracheal epithelia of four ChAT-eGFP mice. We chose these two cell populations, because we anticipated fundamental differences between brush and ciliated cells due to their distinct functions and morphology. We identified ChAT-eGFP positive BC by their green fluorescence and ciliated cells by their beating cilia (Figure 1A). Unbiased analysis using principal component analysis (PCA) of single cells delineated ChAT-eGFP-positive BC and ciliated cells (Figure 1B) identified them as two distinct cell populations. To understand the functional state of the different clusters, we determined the set of genes specific to each cell group using the "single-cell differential expression" (SCDE) approach[29] and all differentially expressed genes with $P < .05$ where displayed in a heatmap (Figure 1C; Table S1). One cell did not cluster with brush or ciliated cells and was excluded from SCDE analysis accordingly. In total, 185 genes were differentially high expressed in ciliated cells and 234 genes in BC. Investigation of differentially expressed genes in ChAT-eGFP-positive cells and ciliated cells revealed expression of the canonical bitter taste signaling components *Tas2r108* and *Trpm5*, in addition to *Chat* and the markers *Avil*, *Dclk1, Sox9,* and *Pou2f3*. Those were among the top hundred most abundant transcripts in BC, whereas others, for example, the ciliated cell marker *Foxj1*, were confined to ciliated cells (Figure 1C; Tables S1 and S2). Interestingly, *Il-25*

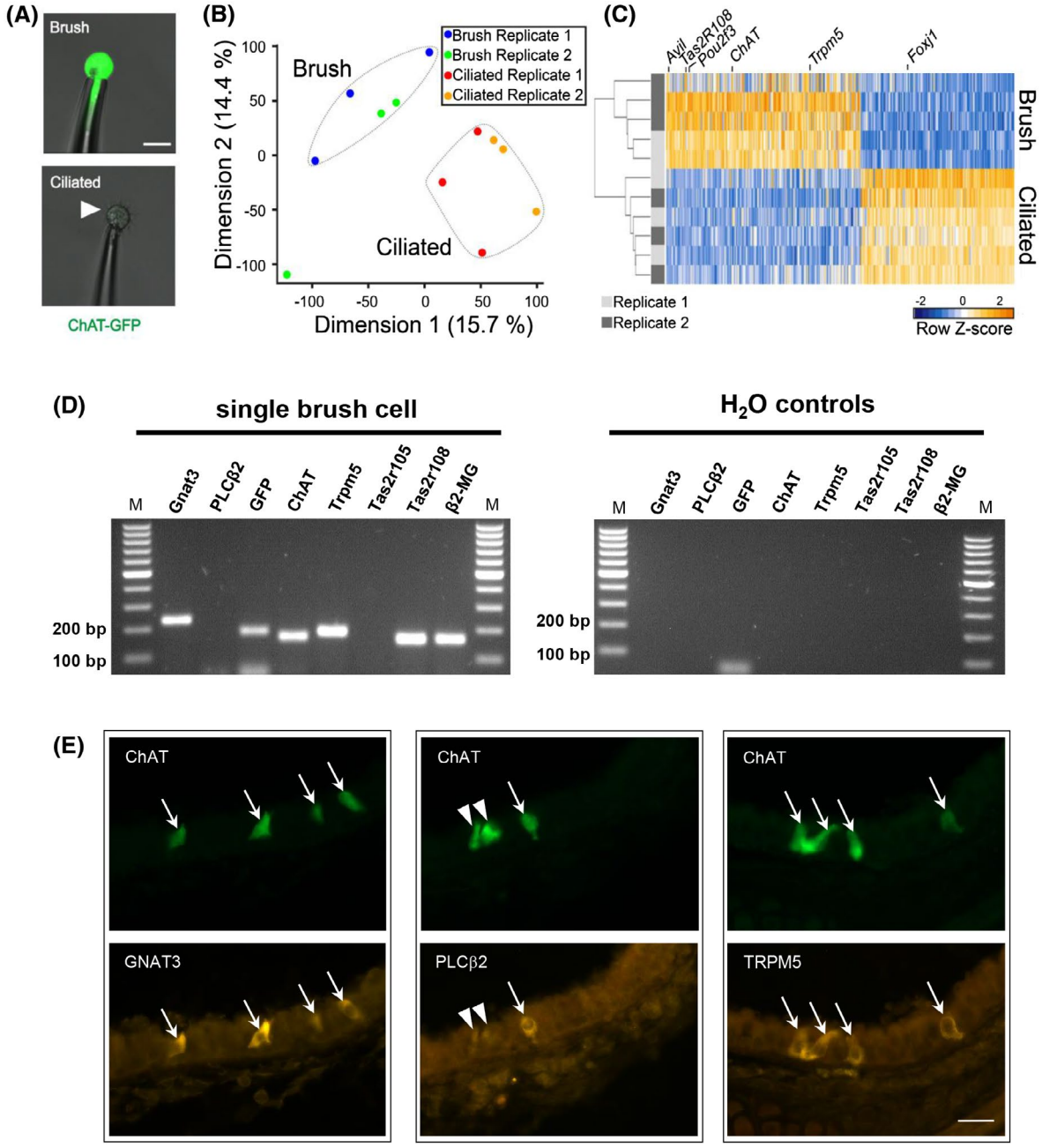

FIGURE 1 Single-cell RNA-seq of ChAT-eGFP expressing brush cells (BC) vs ciliated cells. A, Fluorescent images show collection of BC (eGFP-fluorescent) and ciliated cells (beating cilia, white arrow) using a patch-pipette. B, Scatter plot displaying the first two principal components (PCA) of BC and ciliated cells (dashed lines). Colors indicate cellular identities and replicate as identified by the initial sorting strategy. C, Heatmap displaying transcriptional profiles of 5 brush vs 6 ciliated cells identified by PCA analysis (panel B). D, Single-cell RT-PCR of isolated BC for candidate genes. GFP and β-microglobulin served as positive controls and H_2O controls as negative controls. E, Immunohistochemistry of tracheal sections. Confirmation of the presence of taste signaling proteins in BC (arrows). A subgroup of ChAT-eGFP$^+$ cells was not labeled for PLCβ2 (arrowheads). Scale bar = 20 μm

was not among the gene transcripts enriched in cholinergic BC (Table S2) in contrast to Bankova et al[4] In line with the single-cell RNA-seq data, single-cell RT-PCR experiments revealed brush cell-specific expression of *Tas2r108*, *Gnat3,* and *Trpm5* (Figure 1D). Despite the very high expression of *Plcβ2* in most of the sequenced BC, *Plcβ2* was absent in all BC (Figure S2; Figure 1D). GNAT3-, TRPM5-, and PLCβ2-immunoreactivity was detected only in BC supporting our RNA-seq findings. All ChAT-eGFP-positive cells were labeled for GNAT3 and TRPM5. PLCβ2 was found only in a subpopulation of ChAT-eGFP cells in the tracheal epithelium (Figure 1E). In total, 26 Tas2R were found in our RNA-seq analysis, whereby each brush cell expresses several Tas2R subtypes (Figure S2). Thus, BC are equipped with

the machinery to recognize bitter substances that may have bacterial origin, which might activate cholinergic signaling, as shown for taste buds.[13] We addressed this hypothesis by performing functional experiments.

3.2 | Tracheal BC release ACh

We have previously shown that tracheal BC are chemosensors monitoring innate immunity by triggering protective reflexes to bacterial products including QSM.[4,25] We proposed that BC elicit local responses through paracrine signaling mechanisms on neighboring cells mediated by ACh, since cholinergic inhibition abolished the protective effects. Here, we investigate whether tracheal BC are indeed the source for ACh and release ACh upon stimulation by measuring changes in $[Ca^{2+}]_i$ of freshly dissociated BC or intact tracheae using M3R-expressing CHO-cells as ACh-biosensor. For stimulation we chose denatonium, a potent ligand of Tas2R including Tas2R108,[31] which was identified as a hallmark gene of tracheal BC from our single-cell RNA-seq experiments.

M3R-expressing CHO cells responded to stimulation with ACh with a significantly increased $[Ca^{2+}]_i$ (*$P < .05$ for 1 µmol/L and ***$P < .001$ for 10 µmol/L) (Figure 2A). Increasing concentrations of denatonium did not alter $[Ca^{2+}]_i$ in ACh-sensor cells (Figure 2B). The sensitivity to ACh and the lack of sensitivity to denatonium qualified the M3R-expressing CHO cells as ACh-sensor cells for subsequent experiments. BC showed a dose-dependent rise of $[Ca^{2+}]_i$ in response to increasing denatonium concentrations (Figure 2C). 10 nmol/L and 100 nmol/L denatonium did not evoke a significant change in $[Ca^{2+}]_i$, but 1 mmol/L as well as 12.5 mmol/L denatonium significantly increased $[Ca^{2+}]_i$ (**$P < .01$ and ***$P < .001$, respectively). Upon this positive validation, we investigated if there was a denatonium-induced ACh-release from freshly isolated BC randomly positioned in the vicinity of ACh-sensor cells. In BC, $[Ca^{2+}]_i$ rose in response to denatonium (1 mmol/L), which was followed by a delayed significant increase in $[Ca^{2+}]_i$ in ACh-sensor cells (Figure 2D). The denatonium-evoked increase in $[Ca^{2+}]_i$ was completely abolished in BC and ACh-sensor cells in the presence of the PLCβ2 inhibitor U73122 (Figure 2E) and prominently reduced after application of the Trpm5 inhibitor TPPO (Figure 2F), both crucial steps in the taste transduction cascade in the taste bud. This suggests that the denatonium-induced activation of BC is mediated by the canonical bitter taste signaling pathway. Next, we verified whether the activation of ACh-sensor cells is indeed due to ACh-release from BC. In the presence of the general MR antagonist atropine, the denatonium-induced $[Ca^{2+}]_i$ response in BC was significantly decreased (Figure 2G,H) but completely abolished in ACh-sensor cells (Figure 2G). Thus, the activation of TasR induces ACh-release from BC that in principle is capable of initiating paracrine signaling on neighboring cells (Figure 2I).

In order to exclude effects due to the dissociation of the epithelial cells, we performed $[Ca^{2+}]_i$-imaging experiments in intact ChAT-eGFP mouse tracheae with ACh-sensor cells positioned closely to them (Figure 3A). These experiments confirmed that stimulation with denatonium (1 mmol/L) triggered an increased $[Ca^{2+}]_i$ in BC followed by a time delayed increase in $[Ca^{2+}]_i$ in ACh-sensor cells (Figure 3B). Furthermore, we observed no increase in $[Ca^{2+}]_i$ in ACh-sensor cells upon stimulation with denatonium when they were coincubated with tracheas from *Trpm5*$^{-/-}$ mice in contrast to a coincubation with tracheas from wild-type mice (Figure 3 C-E). Epithelial cells with the morphological appearance of ciliated cells showed a moderate fluctuation in $[Ca^{2+}]_i$ levels which was suggestive for paracrine signaling originating for brush cell activation (Figure 3B). In order to exclude that the activation of ciliated cells is due to spreading of the Ca^{2+}-signal between cell populations due to gap junctions we proved for BC-mediated cholinergic paracrine signaling using dissociated tracheal epithelial cells instead of ACh-sensor cells. Denatonium (12.5 mmol/L) increased $[Ca^{2+}]_i$ in brush cells and in ciliated cells (Figure 3F). Two different populations of ciliated cells could be distinguished, one population sensitive to cholinergic inhibitors and an insensitive population. Conclusive with our single-cell sequencing data, it appears that there are at least two different ciliated cell populations with different expression of MRs, since all analyzed ciliated cells showed a differentially higher expression of the M3R (Figure S3). Accordingly they are expected to show different sensitivities to ACh. The increase in $[Ca^{2+}]_i$ in the first ciliated cell population was inhibited by the MR and nAChR antagonists atropine and mecamylamine (Figure 3G) indicating a stimulation of these cells due to cholinergic signaling evoked by ACh-release from BC. The less pronounced increase in $[Ca^{2+}]_i$ of the other ciliated cell population was not influenced by cholinergic inhibition and suggests the presence of active Tas2R with lower affinity to denatonium in those cells.

3.3 | Denatonium and *Pseudomonas aeruginosa* QSM enhance the transport speed of particles on the tracheal surface dependent on Trpm5 and cholinergic signaling

Next, we investigated whether ACh mediates changes in MC. Application of ACh significantly increased PTS over the complete period of stimulation (Figure 4A). This response was inhibited with the general MR inhibitor atropine (Figure 4A) and with the specific M3R inhibitor 4-DAMP suggesting that the ACh-triggered MC is mediated by the M3R (Figure 4B). Supportively, the response to ATP used as a noncholinergic control stimulus of PTS was not influenced by these inhibitors. Additionally, the bitter substance denatonium significantly

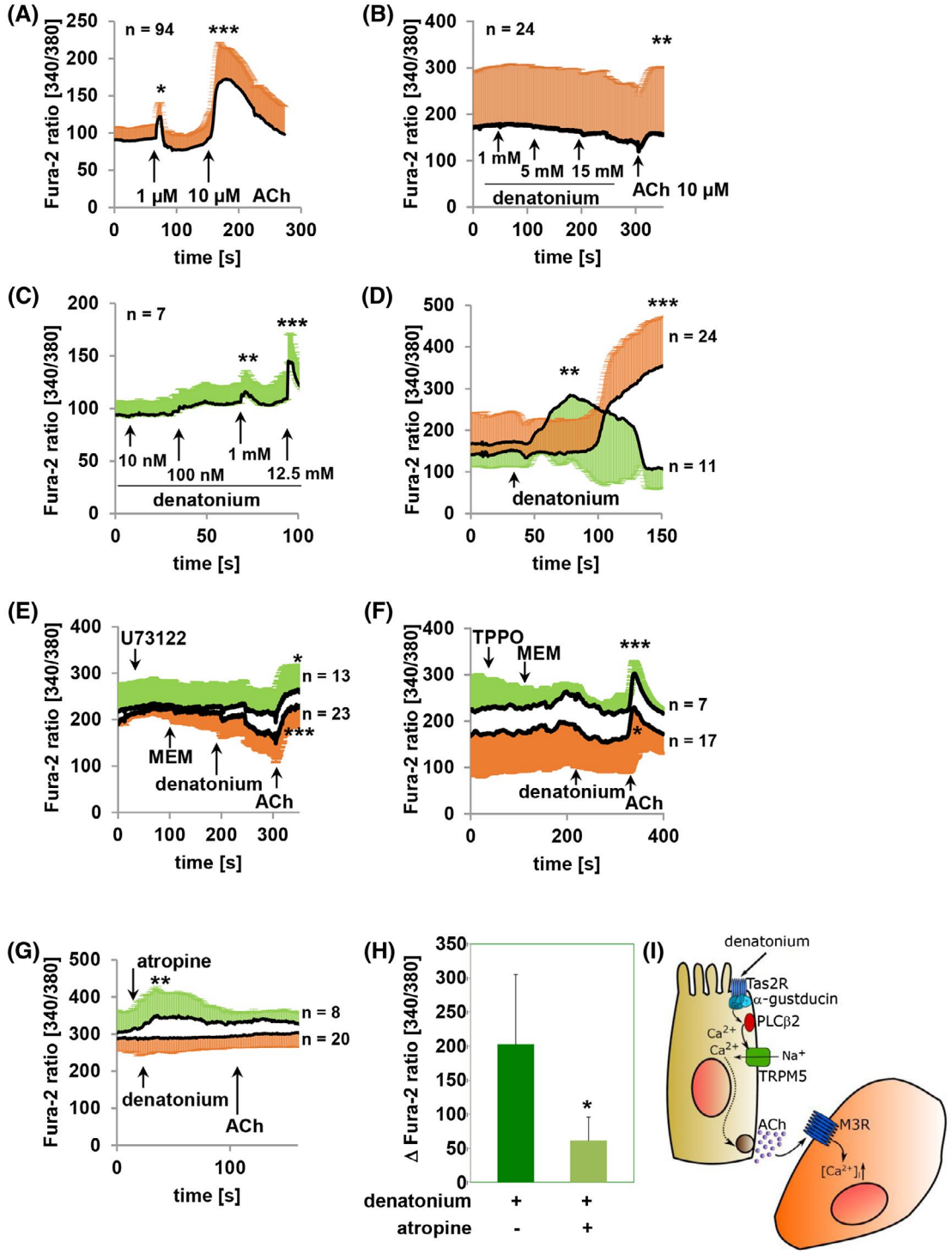

FIGURE 2 Ca^{2+}-imaging experiments of isolated brush cells (BC) (green) and ACh reporter cells (orange). A, Application of ACh evoked a significant increase in $[Ca^{2+}]_i$ in ACh reporter cells. B, Denatonium did not alter $[Ca^{2+}]_i$ in ACh reporter cells, whereas ACh increased $[Ca^{2+}]_i$ significantly. C, In BC, denatonium altered $[Ca^{2+}]_i$ in a concentration-dependent manner. D, Application of denatonium (1 mmol/L) significantly increased $[Ca^{2+}]_i$ in BC followed by a rise in $[Ca^{2+}]_i$ in ACh reporter cells. E, In the presence of the PLCβ2 inhibitor U73122 (10 µmol/L), denatonium (1 mmol/L) had no effect on $[Ca^{2+}]_i$. F, In the presence of the TRPM5 channel inhibitor TPPO, the denatonium-induced rise in $[Ca^{2+}]_i$ was abolished. E-F. ACh (10 µmol/L) served as a positive control. MEM (minimum essential media) was applied as a vehicle control. G, In the presence of the muscarinic ACh receptor inhibitor atropine (50 µmol/L) denatonium (1 mmol/L) still increased $[Ca^{2+}]_i$ in BC, but there was no subsequent rise in $[Ca^{2+}]_i$ in ACh reporter cells. Application of ACh (10 µmol/L) did not affect $[Ca^{2+}]_i$ in the presence of atropine. H, Comparison between the denatonium-induced increase in $[Ca^{2+}]_i$ in BC with and without cholinergic inhibition. A-H. Data represent pooled experiments from at least four different animals and were analyzed with the paired Student's *t* test (A-G) and unpaired Student's *t* test (H). $^*P < .05$, $^{**}P < .01$, $^{***}P < .001$, ns $P > .05$. I, Schematic drawing of the paracrine signaling pathway of tracheal epithelial BC induced by denatonium

increased PTS (Figure 4C). This response was completely abolished in the presence of the general cholinergic receptor inhibitors mecamylamine (nAChR) and atropine (MR) (Figure 4C). Denatonium increased PTS by approx. 45%. The more pronounced increase in PTS induced by ACh can be attributed to the application of the maximum effective dose of ACh (100 µmol/L), whereas denatonium most probably stimulates a release of lower, more physiological concentrations of ACh from BC. Strikingly, the denatonium-induced increase in PTS was absent when the M3R was inhibited with 4-DAMP (Figure 4D) and not changed upon inhibition of gap junctions with carbenoxolone (Figure S4). Consistent with previous

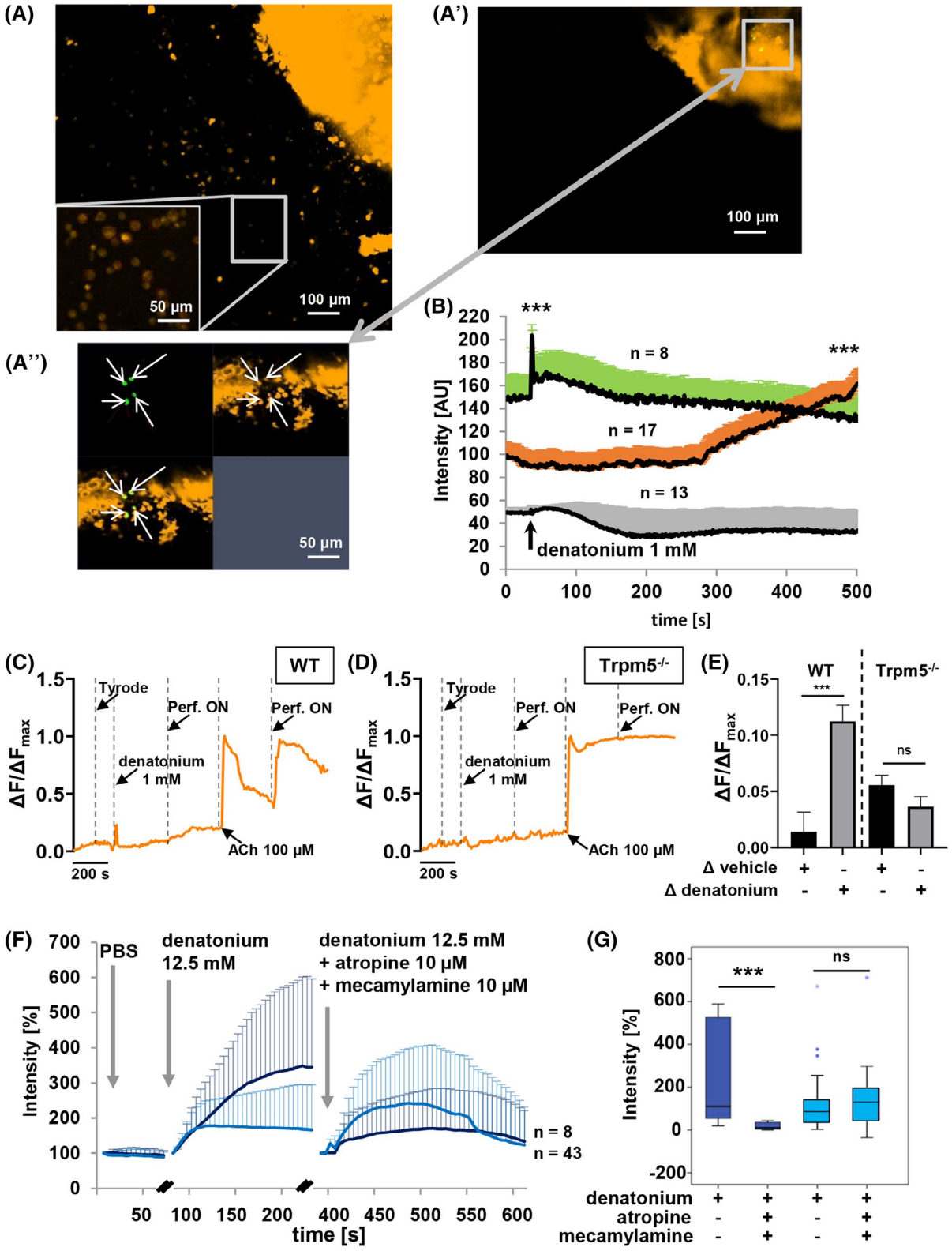

FIGURE 3 Ca^{2+}-imaging experiments of brush cells (BC) and other epithelial cells in intact tracheal slices and reporter cells. A-A′′, A tracheal slice from ChAT-eGFP-mice containing BC (green fluorescence in A′ and A′′) and ciliated cells (orange in A′ and A′′) surrounded by ACh reporter cells (inset in A). All cells were loaded with calcium orange. B, Application of denatonium increased $[Ca^{2+}]_i$ in BC (green curve), which was followed by a rise in $[Ca^{2+}]_i$ in ACh reporter cells (orange curve). Response of other epithelial cells = grey curve. C-D. Ca^{2+}-imaging of ACh-sensor cells in close proximity to intact tracheas. Representive traces for changes in $[Ca^{2+}]_i$ levels in sensor cells. C, Wild-type mice. Application of denatonium increased $[Ca^{2+}]_i$ in sensor cells directly. The increase in $[Ca^{2+}]_i$ in the sensor cell after the perfusion was switched on (Perf. ON) is most probably due to the wash up of the BC-released ACh to the sensor cells. $\Delta F/\Delta F_{max}$: Normalized fura-2 ratio D. *Trpm5*$^{-/-}$ mice. Application of denatonium to the trachea did not change $[Ca^{2+}]_i$ in sensor cells. $\Delta F/\Delta F_{max}$: Normalized fura-2 ratio E. Statistical analyses of data shown in C and D. In sensor cells incubated with tracheas from wild type mice application of denatonium (Δ denatonium) to the tracheas significantly increased $[Ca^{2+}]_i$ when compared with baseline (Δ vehicle). This $[Ca^{2+}]_i$-increase in sensor cells was absent in presence of denatonium-stimulated tracheas from *Trpm5*$^{-/-}$ mice. F. Changes in $[Ca^{2+}]_i$ to stimulation with denatonium of isolated tracheal epithelial cells. An epithelial cell population sensitive to inhibition with cholinergic blockers after BC activation = dark blue (n = 8), an epithelial cell population consisting of cells insensitive to cholinergic anatognists after BC activation = light blue (n = 43). G. Statistical analyses of data shown in (F). For statistical analysis the time points before stimulation and with the maximum response were chosen. Calcium orange intensity after denatonium application without inhibitors vs with inhibitors in ciliated cells that were sensitive to cholinergic inhibitors = dark blue, in ciliated cells that were insensitive to cholinergic inhibitors = light blue. Data were analyzed with the paired Student's *t* test (B, E, G). The y-axis labeling "Intensity" refers to calcium orange intensity pictured in arbitrary units [AU] or percentage [%] (B, F, G).*$P < .05$, **$P < .01$, ***$P < .001$, ns $P > .05$

findings by Droguett et al,[32] the PTS-increase evoked by extracellular ATP applied at the end of each experiment was reduced in the presence of carbenoxolone (Figure S4). Notably, denatonium did not evoke changes in PTS in *Trpm5*$^{-/-}$ mice (Figure 4E) indicating that the denatonium-induced PTS-increase is dependent on ACh released from BC acting in a paracrine manner on ciliated cells. In line with these observations, perfusion of the mucosal surface with denatonium in freely breathing mice in vivo led to a reduction in the respiration rate (Figure S5). This effect was absent when the tracheal epithelium was mechanically removed or the tracheal mucosa was perfused with the cholinergic inhibitor mecamylamine. Additionally, the *P aeruginosa* QSM PQS (Pseudomonas quinolone signal, 2-Heptyl-3-hydroxy-4-quinolone), a multifunctional signaling molecule involved in the regulation of several important virulence factors and a Tas2R-agonist, prominently increased PTS (Figure 4F). This increase was significantly reduced in *Trpm5*$^{-/-}$ mice (Figure 4G). A similar effect was observed also with two other QSM from the same system, 2-AA (2-aminoacetophenone), and DHQ (2,4-dihydroxyquinoline) (Figure S6). Thus, bitter substances and bacterial QSM lead to an activation of the *Trpm5*-dependent signaling cascade present only in BC, which leads to ACh-release and subsequent cholinergic stimulation of mucociliary transport in the lower airways (Figure 4H).

3.4 | MR mediate the autocrine feedback mechanism of released ACh from tracheal BC

In peripheral organs ACh-release is subjected to tight autocrine regulation involving MR.[33] We therefore postulated that ACh-release from BC would also result in an autocrine feedback loop. As observed in our previous experiments (Figure 2C), denatonium increased $[Ca^{2+}]_i$ in isolated tracheal BC from MR wild-type mice ($P < .001$, Figure 5A,K). Intriguingly, the response to denatonium was significantly reduced in the presence of atropine (Figure 5B,K) suggesting that activation of BC might be partly due to a secondary activation of MR in these cells. In BC from *M1R*$^{-/-}$ mice, the denatonium-mediated rise in $[Ca^{2+}]_i$ was significantly smaller than in wild-type mice (Figure 5C,K), indicating that the effect is at least partially mediated by M1R. In the presence of the M3R-specific antagonist 4-DAMP (Figure 5D,K) and in tracheal epithelial BC of *M3R*$^{-/-}$ mice (Figure 5E,K), the denatonium-induced rise in $[Ca^{2+}]_i$ was significantly reduced compared to wild-type mice and comparable to that in *M1R*$^{-/-}$ mice. Inhibition of the M2R with gallamine (Figure 5F,K) increased $[Ca^{2+}]_i$ upon stimulation with denatonium more strongly than in wild-type mice, indicating an inhibitory role of the M2R. The same effect was observed in M2R/M3R-double knockout mice (*M2R/M3R*$^{-/-}$, Figure 5G, K) in which M1R was expressed. Supportive of an autoinhibitory loop of ACh release involving the M2R, the denatonium-induced increase in PTS was significantly increased in the presence of the M2R inhibitor gallamine (Figure 5H) and the M2R was differentially higher expressed in brush cells than in ciliated cells as indicated by our sequencing data (Figure S3). Along with our single-cell RNA-seq results, in which we did not reliably detect the M4R and M5R, the denatonium-induced increase in $[Ca^{2+}]_i$ remained unaltered in *M4R*$^{-/-}$, and *M5R*$^{-/-}$ mice (Figure 5I-K), indicating that the ACh-mediated increase in $[Ca^{2+}]_i$ in BC is mediated by M1R and M3R but not by M4R and M5R (Figure 5K-L).

4 | DISCUSSION

The tracheal epithelium is constantly exposed to inhaled particles and potential pathogens. To prevent infection and

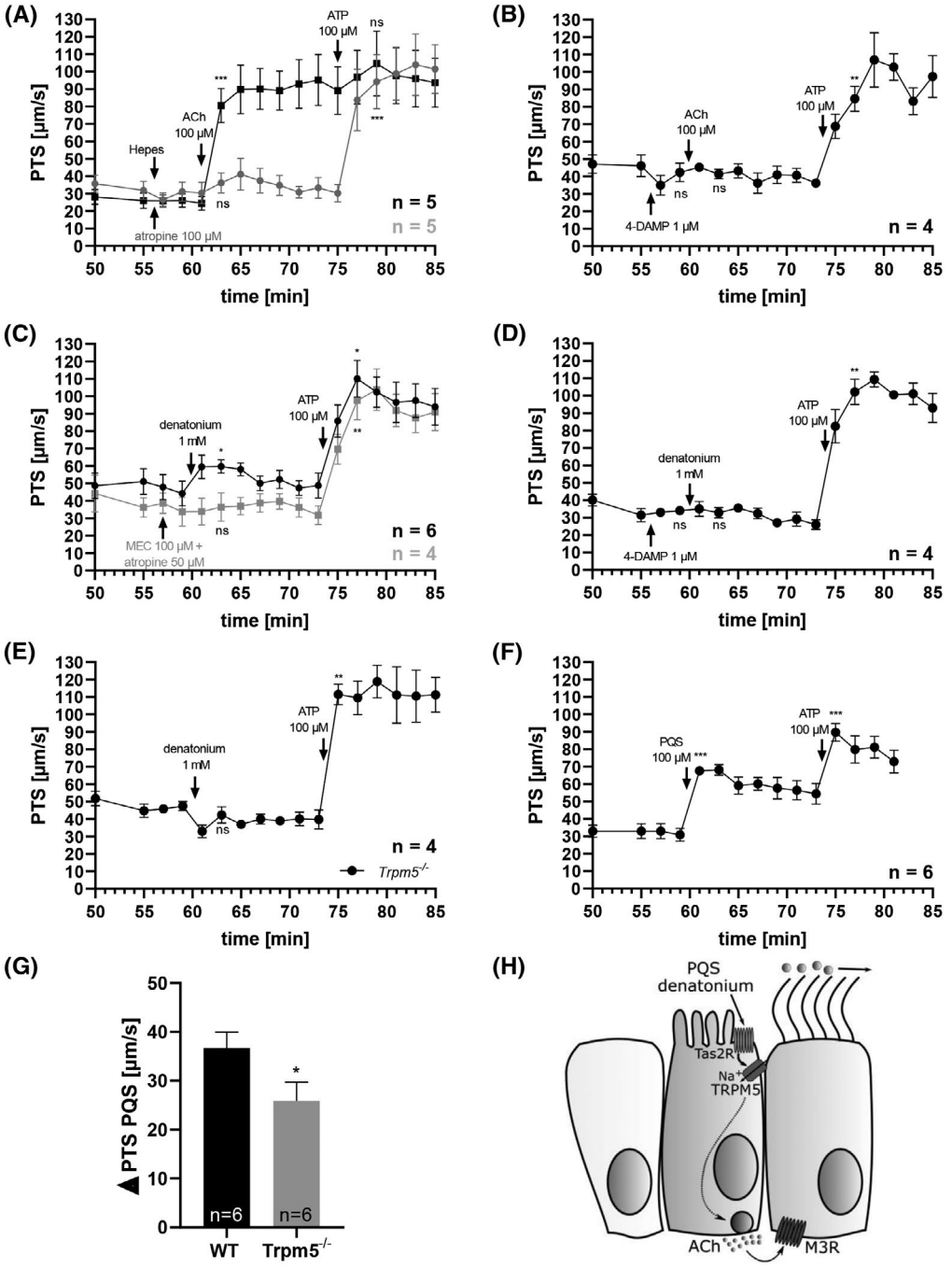

FIGURE 4 Particle transport speed (PTS) measurements of isolated mouse tracheae. A. ACh increased PTS significantly. ATP which was applied as a viability control did not further increase PTS in tracheae from wild-type mice (black line). In the presence of the muscarinic receptor antagonist atropine, ACh had no effect on the PTS, whereas ATP significantly increased PTS (gray line). B. In the presence of the muscarinic ACh-receptor type 3 inhibitor 4-DAMP, ACh had no influence on PTS, whereas ATP significantly increased PTS. C. Denatonium increased PTS significantly (black line). ATP further increased PTS. Denatonium did not influence PTS in the presence of the cholinergic receptor inhibitors mecamylamine (MEC) and atropine (grey line). D. In the presence of 4-DAMP, denatonium had no influence on PTS, whereas ATP significantly increased PTS. E. In *Trpm5*-deficient mice ($Trpm5^{-/-}$) denatonium had no effect on PTS, whereas ATP significantly increased PTS. F. The *Pseudomonas aeruginosa* quorum sensing molecule PQS (Pseudomonas quinolone signal, 2-Heptyl-3-hydroxy-4-quinolon) significantly increased PTS. ATP further increased PTS. A-F. Values before and after application of the substances were compared with the paired Student's *t* test. G. The PQS-induced increase in PTS (ΔPTS) was significantly reduced in $Trpm5^{-/-}$ mice compared to wild-type (WT) mice. Data were compared with the unpaired Student's *t* test. A-G. Data are displayed as mean ± SEM for each animal group. $*P < .05$, $**P < .01$, $***P < .001$, ns $P > .05$. H. Schematic drawing of the proposed model of the activation of mucociliary clearance by tracheal epithelial brush cells in response to bacterial and bitter stimuli. Bitter substances such as denatonium or PQS bind to Tas2R in brush cells (BC), which leads to Trpm5-dependent ACh-release from BC. The released ACh then binds to M3R on neighboring ciliated cells, which subsequently stimulates PTS

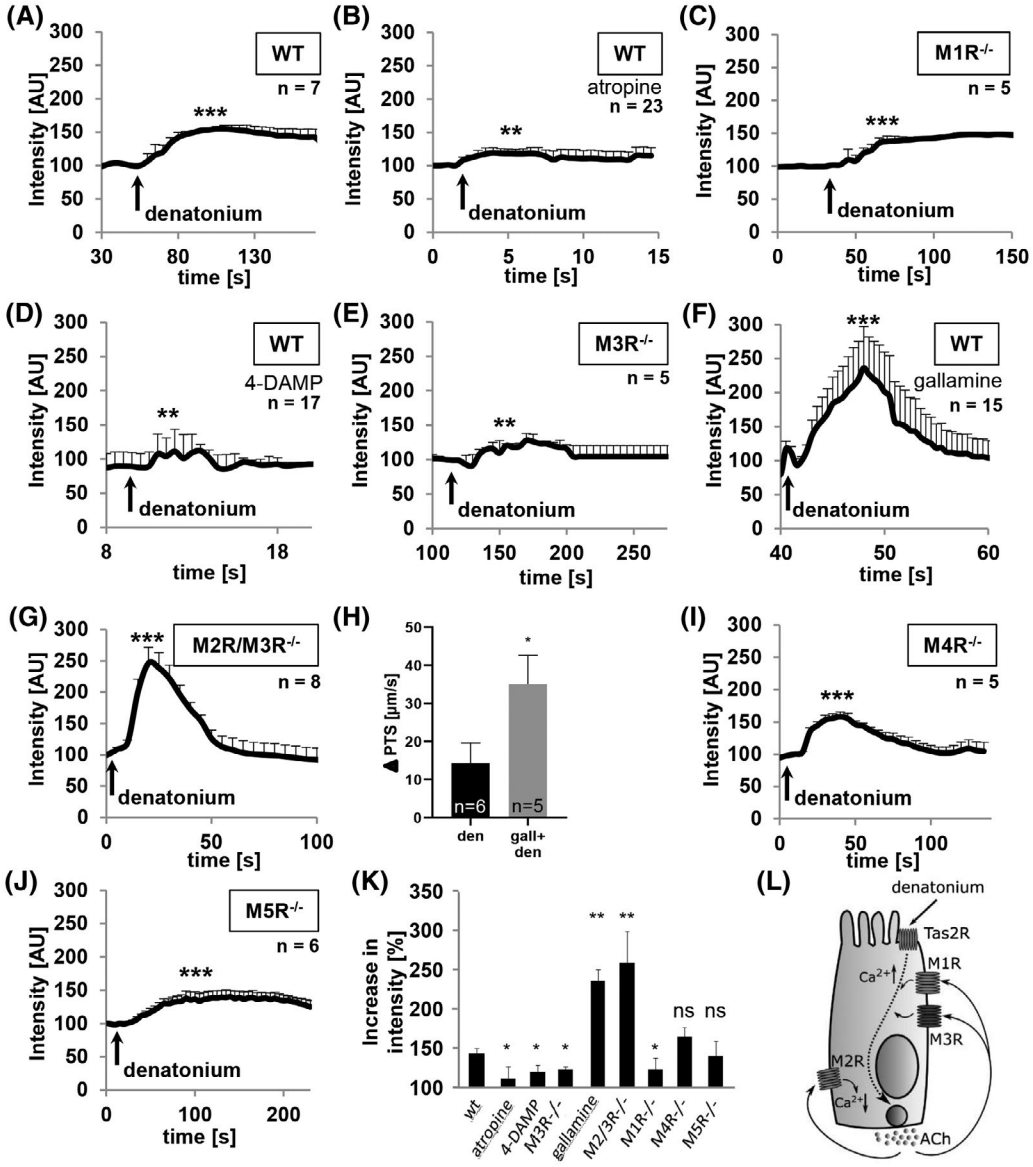

FIGURE 5 Ca^{2+}-imaging experiments of isolated tracheal brush cells (BC). A. In the presence of vehicle (minimal essential medium), denatonium (12.5 mmol/L) significantly increased $[Ca^{2+}]_i$ in BC from wild-type mice. B. In the presence of the muscarinic receptor (MR) inhibitor atropine (50 µmol/L), denatonium significantly increased $[Ca^{2+}]_i$ in BC from wild-type mice. C. In *M1R*-deficient ($^{-/-}$) mice, denatonium evoked a significant rise in $[Ca^{2+}]_i$ in BC. D. In the presence of the M3R blocker 4-DAMP (100 nmol/L), denatonium significantly increased $[Ca^{2+}]_i$ in BC from wild-type mice. E. In $M3R^{-/-}$ mice, denatonium significantly stimulated $[Ca^{2+}]_i$ in BC. F. In the presence of the M2R antagonist gallamine (10 µmol/L), denatonium significantly raised $[Ca^{2+}]_i$ in BC from wild-type mice. G. In $M2R/M3R^{-/-}$ mice, denatonium prominently stimulated $[Ca^{2+}]_i$ in BC. H. Application of gallamine significantly increased the denatonium-induced augmentation of PTS compared to stimulation without the M2R inhibitor. I. In $M4R^{-/-}$ mice, denatonium induced a significant rise in $[Ca^{2+}]_i$ in BC. J. In $M5R^{-/-}$ mice, denatonium significantly increased $[Ca^{2+}]_i$ in BC. K. Bar graph showing the percentage of the increase in $[Ca^{2+}]_i$ intensity after denatonium stimulation in tracheal BC from wild-type (wt) mice with or without different cholinergic blockers or from *MR* genes deficient mouse strains. In $M1R^{-/-}$ and $M3R^{-/-}$ mice as well as in the presence of atropine and 4-DAMP the denatonium-dependent $[Ca^{2+}]_i$ was reduced compared to wild-type mice and comparable among each other. In $M2/3R^{-/-}$ mice and with gallamine the denatonium-evoked $[Ca^{2+}]_i$ was increased compared to wild-type mice and did not differ among each other. In $M4R^{-/-}$ and $M5R^{-/-}$ mice the denatonium-induced increase in $[Ca^{2+}]_i$ was similar to that of wild-type mice. A-K. Maximum responses were used for statistical analysis of all panels. Data are displayed as mean ± SEM for each group. Panels A-G and I-J were analyzed with the paired Student's *t* test. H was analyzed with the unpaired Student's *t* test. Groups shown in K were analyzed with one-way ANOVA followed by Dunnett's multiple comparison test. $*P < .05$, $**P < .01$, $***P < .001$, ns $P > .05$. The *y*-axis labeling "Intensity" refers to calcium orange intensity pictured in arbitrary units [AU] or percentage [%]. L. Schematic drawing of the autocrine cholinergic signaling loop in tracheal epithelial BC. Binding of denatonium to Tas2Rs, for example, Tas2R108, leads to an increased $[Ca^{2+}]_i$ which results in ACh-release from BC. ACh then binds to different MR subtypes present in BC. Binding of ACh to M3R and/or M1R increases $[Ca^{2+}]_i$ in BC, whereas binding of ACh to the M2R inhibits the rise in $[Ca^{2+}]_i$

diseases, several innate immune mechanisms are constantly active in the airways, which help to distinguish between pathogenic and harmless stimuli. A subtype of epithelial cells, so-called BC, were recently identified to harbor taste transduction molecules and cholinergic traits. These cells are able to sense "bitter" tasting bacterial compounds, including QSM and cycloheximide, present in the airway lining fluid. In response to these substances, an epithelium-mediated cholinergic transmission involving activation of nAChR induced aversive reflexes in mice.[7,25] In this study, we investigated the molecular fingerprint of tracheal cholinergic BC and possible mechanisms of cholinergic transmission upon activation by bitter compounds. Two recently published studies identified BC as a distinct population of airway epithelial cells by RNA-seq[9,11] Interestingly, one of these studies distinguished two terminally differentiated brush (= tuft) cell subtypes, both being transient receptor transient receptor potential melastatin 5 channel (*Trpm5)*-positive.[9] However, tuft 1 cells were positive for *Gng13* (G-protein subunit gamma 13) and are likely responsible for taste sensing, whereas tuft 2 cells were *Alox5ap* positive, suggesting leukotriene synthesis. Interestingly, *Chat* was not listed among the marker genes.[9] Notably, Nadjsombati et al,[10] identified *Chat* as a common brush cell marker in *Il-25*-positive tuft cells from several organs. Our RNA-seq analysis and RT-PCR of single *Chat*-positive tracheal epithelial cells revealed expression of *Avil*, *Dclk1*, *Sox9*, *Gnat3*, *Trpm5,* and *Tas2r108* showing that these cells are indeed BC. Out of 35 potential mouse Tas2R (taste receptor type 2) transcripts,[34] we detected 24 in our BC. The cells were equipped with more than one Tas2R as well as with Tas1R3 which characterizes them as polymodal cells in contrast to chemosensory cells in lingual taste buds.[35] Thus, BC are equipped with a potent tool for detection of a broad spectrum of pathogenic molecules due to different receptor combinations. Detection of Tas2R131 and Tas2R143 confirmed the results of previous studies, describing members of the Tas2R143/Tas2R135/Tas2R126 cluster and Tas2R131 in tracheal BC.[24,36] Additionally, we detected high levels of *Gng13* (Guanine nucleotide-binding protein subunit gamma-13) and *Pou2f3* (a transcription factor), which is regulating the generation of different chemosensory cells including tuft cells in the gut and BC in the airways.[37] *Pou2f3* was previously identified as a further marker for tuft 1 cells.[9] Expression levels of *Alox5ap* were lower than *Gng13* in our study.[9] However, since genes of both BC subtypes were enriched in our sequenced *Chat*-positive cells, we cannot allocate them to one of the BC subpopulations. Interestingly, Montoro et al found that tuft 1 cells are also *Il-25*-positive.[9] *Il-25* expressing BC are important for eliciting immune responses in airway diseases including asthma: inhalation of allergens increased BC numbers evoking a BC and *Il-25*-dependent type 2 immune response in the airways.[4] By analogy, gut tuft cells, equivalent to airway BC, are essential for the type 2 immune response fighting parasite infection.[38,39] Notably, these BC were isolated from ChAT-eGFP mice. However, we did not detect *Il-25* but the IL-25 receptor *Il17rb* and genes involved in lipid mediator generation, for example, *Alox5*, *Alox5ap*, *Ltc4s*, *Ptgs1,* and *Pla2g4a* in our cholinergic BC population. Whereas *Tas1r3*, *Tas2r108*, *Tas2r102*, *Tas2r137,* and *Tas2r138* were detected in both studies, we did not find *Tas2R104* and *Tas2R105* and Bankova et al[4] did not find *Tas2r117*, *Tas2r120*, *Tas2r131,* and *Tas2r143*. These differences might be due to differences in the sequencing protocols. Another possibility might be an existence of a non-*Il-25*-expressing cholinergic BC subpopulation. As expected, sequenced ciliated cells expressed the transcription factor *Foxj1*, which is needed for ciliogenesis.[40] Thus, cholinergic tracheal epithelial cells indeed represent a unique cell subtype in the tracheal epithelium.

There is evidence from studies of the nasal epithelium that SCC and microvillous cells respond to appropriate chemical stimuli by ACh-release, thereby activating neighboring and supporting cells, respectively, and evoking local responses and stimulation of sensory nerve fibers, initiating defense mechanisms.[2,6,41-43] Indeed, nose SCC are commonly contacted by peptidergic (CGRP-positive, SP-positive) sensory nerve fibers,[2,7,22,44] whereas only 25% of tracheal BC are in close position to sensory nerve fibers. Stimulation of nasal SCC with denatonium causes SP-mediated neurogenic inflammation dependent on cholinergic transmission,[22] though the direct release of ACh from these cells was not shown. A proof for ACh-release from epithelial cells in a nontaste organ was given for the urethra.[5] In taste buds, ACh alters sensitivity of taste signaling by acting in an autocrine manner via MR.[13] Using ACh-biosensor cells, we demonstrated a release of ACh from tracheal epithelial BC in isolated cells and intact tracheae upon stimulation of the bitter taste signaling cascade. Moreover, we provide direct evidence that ACh-release is dependent on a functional bitter taste signaling cascade since ACh-release was completely abolished with taste transduction cascade inhibitors and not observed in tracheas of *Trpm5*$^{-/-}$ animals. The time-delay in the response of ACh-biosensor cells after stimulation of BC with denatonium is most likely due to time needed for diffusion of the released ACh to the reporter cells. This is further supported by our observation that the sensor cells reacted more strongly after the perfusion was switched on and the ACh released from the BC in the tracheas placed close to them was washed directly onto the sensor cells.

During synaptic transmission, the effect of ACh is terminated very quickly by the enzyme acetylcholine esterase. Since the respiratory epithelium lacks acetylcholine esterase it was proposed that ACh-degradation is slower and thus longer lasting paracrine effects of ACh are expected.[17] In line with this, it is tempting to speculate that accumulation of ACh would lead to inhibition of ACh-release via autocrine signaling, whereas low ACh-concentrations would enhance

ACh-release. We observed that the released ACh subsequently evokes autocrine and paracrine effects. The autocrine effect was mediated by M1R and M3R, whereas M2R inhibited autocrine signaling. We did not find any evidence for an involvement of M4R and M5R. Consistent with these functional observations, the RNA-seq data revealed expression of M1R, M2R, and M3R and no expression for M4R and M5R in BC. Previously, M3R was found to be involved in cholinergic autocrine signaling in lingual taste buds.[4] However, M1R-mRNA was not detected in Type II taste cells and no negative cholinergic feedback loop was found.[4] A negative feedback loop mediated by M2R and M5R in response to bitter substances was reported for urethral BC and a possible role of this loop for bladder overreactivity was suggested.[38] Thus, this negative regulation seems to be specific for the nontaste organs but the involved MR are organ-specific. Here we provide for the first time a proof for a functional negative feedback loop for ACh release from non-neuronal cells. Our RNA-seq data revealed expression of M2R only in brush cells and not in ciliated cells. In line with our findings, in a study from Klein et al,[16] *M2R*$^{-/-}$ mice were found to have an unaltered PTS upon stimulation with muscarine, a general agonist to MR. In this experimental setting muscarine, used in a high dose, most likely activated the predominant M3R present on ciliated cells directly and was masking the response of ACh released additionally from BC. In our study the acute inhibition of M2R in the trachea almost doubled the increase in PTS after stimulation of brush cells with bitter tasting substances. Supportively, the basal PTS in *M2R*$^{-/-}$ mice was enhanced compared to wild-type mice.[16]

Additionally, ACh mediates important innate immune functions after being released from BC, for example, induction of protective respiratory reflexes. We observed a nAChR-dependent decrease in respiratory rate and induction of respiratory events similar to cough reflexes in response to Tas2R-stimulation. This indicates that tracheal epithelial BC act on nearby cholinergic sensory nerve fibers and the released ACh evokes centrally mediated changes in respiration. This is in accordance with our previous studies, showing that "bitter tasting" bacterial substances including cycloheximide and *P aeruginosa* QSM N-3-oxododecanoyl-homoserine lactone induced a protective drop in the breathing frequency which was dependent on nAChR.[7,25]

Another important protective mechanism is activation of MC, the oldest evolutionary mechanism of innate immunity of the airways.[45] MC represents the first step for removing potentially dangerous inhaled particles and bacteria from the airways. Consistent with previous reports,[15,16,46] we have observed that MC is regulated by ACh and that this ACh-induced increase in cilia-driven PTS is M3R-dependent. Here, we provide functional proof that Tas2R agonists, for example, denatonium are capable of inducing an increase in PTS that is Trpm5-dependent and mediated by M3R. Since we have found Trpm5 solely in BC the increase in PTS can only be attributed to a release of ACh from BC. As M3R inhibition completely abolished the denatonium-induced increase in PTS and inhibition of gap junctions did not influence the denatonium-induced rise in PTS, we can exclude that the BC-mediated effect on MC is mediated by NO or by ATP released through gap junctions to the ciliated cells. In human upper airways MC is regulated by the release of NO from ciliated cells after stimulation with bitter and bacterial substances.[47] Since in the upper airways SCC are intensively approached by sensory nerve endings[6] it appears that their protective responses are mainly mediated by cholinergic activation of nerve endings such as an induction of neurogenic inflammation.[22] In the lower airways BC are less frequently innervated by sensory nerve endings,[7] therefore it is likely that they are responsible for local effects mediated by paracrine signaling such as the BC-mediated increase in MC in our study. However, while we provide profound evidence for an essential role of BC regulation of PTS in isolated tracheae, experiments validating BC regulation of MC in vivo are still needed. In addition both chemosensory cells from the upper and lower respiratory tract, SCC and BC, are responsible for cytokine production and regulation of respiration.[2,4,7]

Furthermore, in our study different *P aeruginosa* QSM of the *pqs* system[48] PQS, 2-AA, and DHQ increased PTS and this effect was dependent on Trpm5-signaling in BC. In a recent study, PQS and HHQ were observed to act on several human Tas2R, namely Tas2R4, Tas2R16, Tas2R38, Tas2R39, and Tas2R40, in a HEK293T overexpression system.[49] In cultured airway epithelial cell lines and primary sinonasal air liquid interface cultures PQS increased $[Ca^{2+}]_i$.[49] Interestingly, the strongest response to PQS was observed on human Tas2R4, which is the orthologue to mouse Tas2R108, the receptor that was identified as a marker gene of cholinergic tracheal BC in our RNA-seq analyses. However, the small residual response to PQS in *Trpm5*$^{-/-}$ mice and the detection of Tas2R in ciliated cells in our RNA-seq analyses is indicative for direct effects on ciliated cells. Cilia of human ciliated cells were previously found to be equipped with Tas2R, which modulate ciliary beat frequency independently of canonical taste signaling.[50] It is tempting to speculate that this mechanism is acting complementary to the cholinergic paracrine signaling of BC. Nevertheless, the lack of BC-mediated protective responses to *P aeruginosa* QSM might lead to longer presence of the human pathogen in the airways, where it can cause infections in immune-compromised patients and in patients with cystic fibrosis. Several immune cells can be directly stimulated by ACh. For example, activation of nAChR in monocytes inhibits ATP-induced inflammasome activation by inhibiting IL1β-release.[14,51,52]

In conclusion, the present findings reveal that the whole transcriptome of tracheal epithelial BC is distinct to that

of ciliated cells. BC are cholinergic and predominantly express the components of the bitter taste signaling cascade. Activation of this bitter taste signaling cascade leads to ACh-release from these cells, which subsequently triggers important protective mechanisms of the respiratory tract, including respiratory reflexes and increased MC. We interpret the ACh-release from BC as the first step in the activation of primary innate immune defense mechanisms against inhaled pathogens. This might serve as a novel pharmacological target in the treatment of infectious diseases of the respiratory tract.

ACKNOWLEDGMENTS

The authors thank Tamara Papadakis (Institute for Anatomy and Cell Biology, Justus-Liebig-University Giessen, Germany), Nora Aouragh and Hassan Kanj (Institute for Anatomy and Cell Biology, Saarland University, Germany) for skillful technical assistance and Dr Stephan Maxeiner (Institute of Anatomy and Cell Biology, Saarland University, Germany) for critical reading of the manuscript. We thank Saskia Evers for assistance in in vivo Ca^{2+} imaging in isolated tracheas. We thank Dr P. Scholz and Dr S. Osterloh (Department of Cell Physiology, Ruhr-University Bochum, Germany) for sharing their expertise regarding RNA-seq from primary cells and for providing the photos shown in Figure 1A. We thank Dr Jürgen Wess for providing the muscarinic receptor-deficient mouse strains. The authors declare that no conflicts of interest exist. This work was supported by the German Research Society (DFG SFB TRR 152 project P01 to VF, project P22 to GKC, KR4338/1-1 to GKC) and the Helmholtz Association's Initiative and Networking Fund (AKHH).

AUTHOR CONTRIBUTIONS

IJ, RN, SW, MA, JA, VF, MIH, and GKC performed experiments. IJ, MIH, SA, LL, JV, A-E S, and GKC analyzed the data. MIH, IJ, ME, AKHH, BJC, A-E S, and GKC interpreted the results. GKC conceived the study and MIH and GKC wrote the manuscript.

CONFLICT OF INTEREST

The authors declare no conflict of interest.

REFERENCES

1. Chilvers MA, O'Callaghan C. Local mucociliary defence mechanisms. *Paediatr Respir Rev*. 2000;1:27-34.
2. Tizzano M, Gulbransen BD, Vandenbeuch A, et al. Nasal chemosensory cells use bitter taste signaling to detect irritants and bacterial signals. *Proc Natl Acad Sci*. 2010;107:3210-3215.
3. Xu H, Delling M, Jun JC, Clapham DE. Oregano, thyme and clove-derived flavors and skin sensitizers activate specific TRP channels. *Nat Neurosci*. 2006;9:628-635.
4. Bankova LG, Dwyer DF, Yoshimoto E, et al. The cysteinyl leukotriene 3 receptor regulates expansion of IL-25–producing airway brush cells leading to type 2 inflammation. *Sci Immunol*. 2018;3:eaat9453.
5. Deckmann K, Filipski K, Krasteva-Christ G, et al. Bitter triggers acetylcholine release from polymodal urethral chemosensory cells and bladder reflexes. *Proc Natl Acad Sci*. 2014;111:8287-8292.
6. Finger TE, Bottger B, Hansen A, Anderson KT, Alimohammadi H, Silver WL. Solitary chemoreceptor cells in the nasal cavity serve as sentinels of respiration. *Proc Natl Acad Sci*. 2003;100:8981-8986.
7. Krasteva G, Canning BJ, Hartmann P, et al. Cholinergic chemosensory cells in the trachea regulate breathing. *Proc Natl Acad Sci*. 2011;108:9478-9483.
8. Schütz B, Jurastow I, Bader S, et al. Chemical coding and chemosensory properties of cholinergic brush cells in the mouse gastrointestinal and biliary tract. *Front Physiol*. 2015;6:1-14.
9. Montoro DT, Haber AL, Biton M, et al. A revised airway epithelial hierarchy includes CFTR-expressing ionocytes. *Nature*. 2018;560:319-324.
10. Nadjsombati MS, McGinty JW, Lyons-Cohen MR, et al. Detection of succinate by intestinal tuft cells triggers a type 2 innate immune circuit. *Immunity*. 2018;49:33-41.
11. Plasschaert LW, Žilionis R, Choo-wing R, et al. A single-cell atlas of the airway epithelium reveals the CFTR-rich pulmonary ionocyte. *Nature*. 2018;560:377-381.
12. Tallini YN, Shui B, Greene KS, et al. BAC transgenic mice express enhanced green fluorescent protein in central and peripheral cholinergic neurons. *Physiol Genomics*. 2006;27:391-397.
13. Dando R, Roper SD. Acetylcholine is released from taste cells, enhancing taste signalling. *J Physiol*. 2012;590:3009-3017.
14. Hecker A, Küllmar M, Wilker S, et al. Phosphocholine-modified macromolecules and canonical nicotinic agonists inhibit ATP-induced IL-1β release. *J Immunol*. 2015;195:2325-2334.
15. Hollenhorst MI, Lips KS, Wolff M, et al. Luminal cholinergic signalling in airway lining fluid: a novel mechanism for activating chloride secretion via Ca^{2+}-dependent Cl^- and K^+ channels. *Br J Pharmacol*. 2012;166:1388-1402.
16. Klein MK, Haberberger RV, Hartmann P, et al. Muscarinic receptor subtypes in cilia-driven transport and airway epithelial development. *Eur Respir J*. 2009;33:1113-1121.
17. Kummer W, Lips KS, Pfeil U. The epithelial cholinergic system of the airways. *Histochem Cell Biol*. 2008;130:219-234.
18. Lee RJ, Kofonow JM, Rosen PL, et al. Bitter and sweet taste receptors regulate human upper respiratory innate immunity. *J Clin Invest*. 2014;124:1393-1405.
19. Lee RJ, Xiong G, Kofonow JM, et al. T2R38 taste receptor polymorphisms underlie susceptibility to upper respiratory infection. *J Clin Invest*. 2012;122:4145-4159.
20. Myers EN, Runer T, Cervin A, Lindberg S, Uddman R. Nitric oxide is a regulator of mucociliary activity in the upper respiratory tract. *Otolaryngol – Head Neck Surg*. 1998;119:278-287.
21. Yan CH, Hahn S, McMahon D, et al. Nitric oxide production is stimulated by bitter taste receptors ubiquitously expressed in the sinonasal cavity. *Am J Rhinol Allergy*. 2017;31:85-92.
22. Saunders CJ, Christensen M, Finger TE, Tizzano M. Cholinergic neurotransmission links solitary chemosensory cells to nasal inflammation. *Proc Natl Acad Sci*. 2014;111:6075-6080.
23. Kaske S, Krasteva G, König P, et al. TRPM5, a taste-signaling transient receptor potential ion-channel, is a ubiquitous signaling component in chemosensory cells. *BMC Neurosci*. 2007;8:49.
24. Liu S, Lu S, Xu R, et al. Members of bitter taste receptor cluster Tas2r143/Tas2r135/Tas2r126 are expressed in the epithelium of murine airways and other non-gustatory tissues. *Front Physiol*. 2017;8:1-17.

25. Krasteva G, Canning BJ, Papadakis T, Kummer W. Cholinergic brush cells in the trachea mediate respiratory responses to quorum sensing molecules. *Life Sci*. 2012;91:992-996.
26. Martin M. Cutadapt removes adapter sequences from high-throughput sequencing reads. *EMBnet.Journal*. 2011;17:10-12.
27. Dobin A, Davis CA, Schlesinger F, et al. STAR: ultrafast universal RNA-seq aligner. *Bioinformatics*. 2013;29:15-21.
28. Trapnell C, Williams BA, Pertea G, et al. Transcript assembly and quantification by RNA-Seq reveals unannotated transcripts and isoform switching during cell differentiation. *Nat Biotechnol*. 2010;28:511-515.
29. Kharchenko PV, Silberstein L, Scadden DT. Bayesian approach to single-cell differential expression analysis. *Nat Methods*. 2014;11:740-742.
30. König P, Krain B, Krasteva G, Kummer W. Serotonin increases cilia-driven particle transport via an acetylcholine-independent pathway in the mouse trachea. *PLoS ONE*. 2009;4:1-7.
31. Chandrashekar J, Mueller KL, Hoon MA, et al. T2Rs function as bitter taste receptors. *Cell*. 2000;100:703-711.
32. Droguett K, Rios M, Carreño DV, et al. An autocrine ATP release mechanism regulates basal ciliary activity in airway epithelium. *J Physiol*. 2017;595:4755-4767.
33. Fryer AD, Jacoby DB. Effect of inflammatory cell mediators on M2muscarinic receptors in the lungs. *Life Sci*. 1993;52:529-536.
34. Lossow K, Hübner S, Roudnitzky N, et al. Comprehensive analysis of mouse bitter taste receptors reveals different molecular receptive ranges for orthologous receptors in mice and humans. *J Biol Chem*. 2016;291:15358-15377.
35. Roper SD, Chaudhari N. Taste buds: cells, signals and synapses. *Nat Rev Neurosci*. 2017;18:485-497.
36. Krasteva-Christ G, Soultanova A, Schütz B, et al. Identification of cholinergic chemosensory cells in mouse tracheal and laryngeal glandular ducts. *Int Immunopharmacol*. 2015;29:158-165.
37. Yamashita J, Ohmoto M, Yamaguchi T, Matsumoto I, Hirota J. Skn-1a/Pou2f3 functions as a master regulator to generate Trpm5-expressing chemosensory cells in mice. *PLoS ONE*. 2017;12:e0189340.
38. Gerbe F, Sidot E, Smyth DJ, et al. Intestinal epithelial tuft cells initiate type 2 mucosal immunity to helminth parasites. *Nature*. 2016;529:226-230.
39. Howitt MR, Lavoie S, Michaud M, et al. Tuft cells, taste-chemosensory cells, orchestrate parasite type 2 immunity in the gut. *Science*. 2016;351:1329-1333.
40. You Y, Huang T, Richer EJ, et al. Role of f-box factor foxj1 in differentiation of ciliated airway epithelial cells. *Am J Physiol Cell Mol Physiol*. 2004;286:L650-L657.
41. Finger TE, Kinnamon SC. Taste isn't just for taste buds anymore. *F1000 Biol Rep*. 2011;3:1-7.
42. Fu Z, Ogura T, Luo W, Lin W. ATP and odor mixture activate TRPM5-expressing microvillous cells and potentially induce acetylcholine release to enhance supporting cell endocytosis in mouse main olfactory epithelium. *Front Cell Neurosci*. 2018;12:1-16.
43. Ogura T, Szebenyi SA, Krosnowski K, Sathyanesan A, Jackson J, Lin W. Cholinergic microvillous cells in the mouse main olfactory epithelium and effect of acetylcholine on olfactory sensory neurons and supporting cells. *J Neurophysiol*. 2011;106:1274-1287.
44. Luciano L, Reale E, Ruska H. Über eine "chemorezeptive" Sinneszelle in der Trachea der Ratte. *Zeitschrift für Zellforsch und Mikroskopische Anat*. 1968;85:350-375.
45. Bakshani CR, Morales-Garcia AL, Althaus M, et al. Evolutionary conservation of the antimicrobial function of mucus: a first defence against infection. *NPJ Biofilms Microbiomes*. 2018;4:1-12.
46. Schmid A, Salathe M. Ciliary beat co-ordination by calcium. *Biol Cell*. 2011;103:159-169.
47. Carey RM, Lee RJ. Taste receptors in upper airway immunity. *Nutrients*. 2019;11:1-17.
48. Allegretta G, Maurer CK, Eberhard J, et al. In-depth profiling of MvfR-regulated small molecules in pseudomonas aeruginosa after quorum sensing inhibitor treatment. *Front Microbiol*. 2017;8:1-12.
49. Freund JR, Mansfield CJ, Doghramji LJ, et al. Activation of airway epithelial bitter taste receptors by Pseudomonas aeruginosa quinolones modulates calcium, cyclic-AMP, and nitric oxide signaling. *J Biol Chem*. 2018;293:9824-9840.
50. Shah AS, Ben-Shahar Y, Moninger TO, Kline JN, Welsh MJ. Motile cilia of human airway epithelia are chemosensory. *Science*. 2009;325:1131-1134.
51. Richter K, Mathes V, Fronius M, et al. Phosphocholine-an agonist of metabotropic but not of ionotropic functions of α9-containing nicotinic acetylcholine receptors. *Sci Rep*. 2016;6:1-13.
52. Richter K, Sagawe S, Hecker A, et al. C-reactive protein stimulates nicotinic acetylcholine receptors to control ATP-mediated monocytic inflammasome activation. *Front Immunol*. 2018;9.

SUPPORTING INFORMATION

Additional supporting information may be found online in the Supporting Information section.

How to cite this article: Hollenhorst MI, Jurastow I, Nandigama R, et al. Tracheal brush cells release acetylcholine in response to bitter tastants for paracrine and autocrine signaling. *The FASEB Journal*. 2020;34:316–332. https://doi.org/10.1096/fj.201901314RR